SLAC-PUB-95-6132
JUNE 1995

Precision Magnet Movers for the Final Focus Test Beam

G. BOWDEN, P. HOLIK, AND S. R. WAGNER*

Stanford Linear Accelerator Center
Stanford University, Stanford, California 94309

and

G. HEIMLINGER AND R. SETTLES

Max-Plank-Institut für Physik, Werner-Heisenberg-Institute

Föhringer Ring 6, D-80805 München

ABSTRACT

Fully automated movers capable of positioning beamline magnets weighing more than 100 kg to a few microns over several millimeters have been designed and built for the Final Focus Test Beam at SLAC. These movers also provide incremental motion as small as a few tenths of a micron. We review the basic design considerations, the hardware realization of the movers, and the extensive tests conducted on these electromechanical stages. Suggestions for the improvement and augmentation of such movers are also given.

Submitted to *Nuclear Instruments and Methods A*

* Work supported by the Department of Energy, contract DE-AC03-76SF00515.

1. Introduction

A future linear collider will be required to achieve e^+e^- collisions at energies above those accessible at LEP 200 ($E_{cm} > 200$ GeV) in a cost efficient fashion.[1] As opposed to storage rings, which produce luminosity by having the particle bunches undergo repeated collisions, linear colliders produce luminosity in large part by making beam densities as high as possible, and therefore the transverse areas of the beams as small as possible, at their interaction point (IP). At the only existing linear collider, the SLAC Linear Collider (SLC), the transverse dimensions of the beams at the IP are on the order of 1 μm. This results in alignment tolerances for certain critical magnets in the SLC final focus on the order of 10 μm, and for magnets and beam position monitors (BPMs) in the linac on the order of 100 μm. All current designs for higher energy linear colliders have even smaller transverse beam dimensions at their IPs, and some designs have vertical beam sizes at the IP on the order of a few *nanometers*. This implies alignment tolerances of about 10 μm on linac components and ≤ 1 μm for certain critical magnets in the final focus. This paper will describe the design, construction, and testing of automated magnet movers to meet this need.

As with the SLC, the next generation linear colliders will consist of e^+ and e^- sources, damping rings, bunch compressors, linacs comprised of power sources (klystrons and modulators) feeding r.f. structures, and final focuses. However, virtually all of these components will need to be significantly more advanced than those currently in use on the SLC. For this reason, there is an active program of linear collider research and development currently underway at accelerator laboratories around the world. One of these projects is the Final Focus Test Beam (FFTB) at SLAC.[2,3]

The design goal of the FFTB is to transport a low emittance electron beam from the SLAC linac and demagnify it by a factor of 380 to a transverse spot size of 1 μm horizontal by 60 nm vertical. This is a comparable demagnification to that needed in a next linear collider (NLC) final focus. The smaller spot sizes

needed by the NLC will be achieved with a similar final focus and smaller beam emittances. This demagnification requires a full second-order chromatic correction. This is achieved with 28 quadrupole magnets and four sextupole magnets between the linac and the final doublet. The movers described in this paper were built for these magnets.

The final alignment of these magnets is performed with the beam itself. Beam trajectories are measured by high precision beam position monitors (BPMs)[4] located inside and between the magnets. The effects of misaligned magnets can be observed in these trajectories, and the magnets are then remotely moved to center them on the desired beamline. Some of the magnets have transverse alignment tolerances of ~ 1 μm, but since the magnets are short (45 cm), alignment tolerances are much looser for pitch and yaw than for x, y or roll (α).[5] The movers described here are remotely adjustable in transverse position with pitch and yaw constrained by mechanical tolerances. Large scale application of beam based alignment at the μm level requires a mover mechanism which can smoothly produce small incremental motions using inexpensive components in a low tolerance design.

2. Basic Design

2.1 Mover Mechanism

The FFTB magnet movers differ from conventional positioning stages used in instruments and machine tools. The design takes advantage of requirements which are unique to magnet positioners. Position control needs relatively high resolution (≤ 1 μm) but the motion range will be limited to ~ 1 mm. Adjustment of angular alignment as well as translation is needed but the motions need not be orthogonal or linear since computer control systems can be adapted to unusual geometries. These movers are designed to compensate for thermal or geological disturbances with time constants of hours and days. They are not designed to correct for rapid mechanical or seismic vibrations with time constants of seconds

or less. However, the speed of adjustment needs to be sufficiently fast (on the order of a minute) so that the process of beam-based alignment is not cumbersomely slow. The mechanics must be able to support loads exceeding 1 ton but should have smooth hysteresis-free motion at the micron level. The design must be simple and reliable enough for large scale use where hundreds of magnets need remote positioning. For this application conventional precision crossed-slide-leadscrew-positioning stages are costly and require protection against beyond-range motion. High resolution piezioelectric positioners[6] have limited range and require feedback stabilization against drift.

The remote magnet positioning mounts used in the FFTB kinematically support the magnets on roller cams. The magnet rests under gravity in a cradle formed by the cams as shown in Fig. 1.

This type of kinematic support is similar to the 'Kelvin Clamp'[7] used in laboratory optics and instrumentation. 'V' blocks and flat planes fixed to the magnet make point or line contact with the outer bearing races of the roller cams. Rotation of the eccentric shafts inside the roller cams shifts the magnet position. This type of kinematic support where the number of contact points balances the number of degrees of spatial freedom has the advantage of avoiding all free play between magnet and mount. The magnet always remains in contact with each of the supporting cams regardless of its position. No precise mechanical dimensions are needed to insure zero play. No clamping forces other than gravity can distort the magnet's shape. The magnet can be removed from the mount and replaced without realignment. During operation, only the inner eccentric shaft of a support cam rotates under motor control. The outer cam bearing race remains fixed in contact with the magnet as shaft rotation lifts the magnet. In such a system, failures of the control system will only cause the cam to cycle around again. Magnet motions are strictly bounded by the design geometry. Limit switches are not needed for over-travel protection. All support cams are arranged so that gravity applies a load torque to each camshaft drive train. This torque removes all backlash except at the extreme of cam lift. All parts move by pure rolling motion and are free of

hysteresis from intermittent and reversing sliding motion.

This mount can adjust the horizontal and vertical position of the magnet as well as the magnet's roll angle around the beam axis. The magnet's longitudinal position along the beam line as well as its alignment to the beam direction in pitch and yaw are fixed in the support mount and not remotely adjustable. Figure 2 shows the 3-motor positioning mount used to support FFTB quadrupole magnets. Figure 3 is a photograph of two movers, with the quadrupole magnets they support, installed on the FFTB beamline.

2.2 Equations of Motion

A position control system based on roller cams requires equations relating the magnet's position and orientation $\vec{x}_{MAG} = (x, y, \alpha)$ to the camshaft angles $\vec{\theta}_{CAM} = (\theta_1, \theta_2, \theta_3)$. The transformation and its inverse can be derived from the geometry of the mechanism. All three shaft angles are coupled to all three magnet position variables by nonlinear trigonometric functions. For the three-cam FFTB positioner with cam radius R and cam lift L :

$$x_1 = x + a\cos\alpha + b\sin\alpha - a, \tag{1.1}$$

$$y_1 = y - b\cos\alpha + a\sin\alpha + c, \tag{1.2}$$

$$\beta_\pm = \frac{\pi}{4} \pm \alpha, \tag{1.3}$$

$$\theta_1 = \alpha - \sin^{-1}\Big(\frac{1}{L}\big((x_1 + S_2)\sin\alpha - y_1\cos\alpha + (c - b)\big)\Big), \tag{1.4}$$

$$\theta_2 = \alpha - \sin^{-1}\Big(\frac{1}{L}\big((x_1 + S_1)\sin\beta_- + y_1\cos\beta_- - R\big)\Big), \tag{1.5}$$

$$\theta_3 = \alpha - \sin^{-1}\Big(\frac{1}{L}\big((x_1 - S_1)\sin\beta_+ - y_1\cos\beta_+ + R\big)\Big). \tag{1.6}$$

The origin of the magnet coordinate system, $\vec{x}_{MAG} = (x, y, \alpha) = (0, 0, 0)$, is referred to as the mover "midrange" position. The origins of this coordinate system,

the intermediate (x_1, y_1) coordinate system, and the design dimensions a, b, c, R, L, S_1, and S_2 are shown in Fig. 1. With the magnet at its midrange position, the cam phase angles, measured counterclockwise from the x axis, are $(\theta_1^0, \theta_2^0, \theta_3^0) = (0°, 135°, 45°)$. The $\vec{\theta}_{CAM}$ given in Eq. 1 are with respect to these angles.

2.3 Range of Motion

The range of motion of these movers encloses a volume in $\vec{x}_{MAG}$ space, as shown in Fig. 4. For $\alpha = 0$ the accessible region for x and y is shown in Fig. 5a. The maximum value for x can only be achieved when $y = 0$ and is $x_{MAX} = \sqrt{2}L$. The maximum value for y can be achieved for many but not all accessible values of x and is $y_{MAX} = L$. For $\alpha = 1000$ μrad (Fig. 5b) the symmetry of the accessible area has been broken. The maximum and minimum accessible values for y have moved up, and the largest accessible values for x have shifted down and to the left. For a roll of equal magnitude but opposite sign, the accessible region for the positive value of α undergoes a parity transformation $\big((x, y) \rightarrow (-x, -y)\big)$. By $\alpha = 5000$ μrad (Fig. 5c) the accessible area has become a triangle, and by $\alpha = 9550$ μrad (Fig. 5d) the accessible region starts to lose the origin. The maximum accessible value of α is about 13200 μrad, achievable only in a small region far from the origin; for the $R = 31.0$ mm, $L = 1.5875$ mm we used, this area is near $(-1190\mu\text{m}, +320\mu\text{m})$.

2.4 More Degrees of Freedom

Kinematic roller cam supports can be applied to a variety of geometries. Figure 6 shows a barrel containing the final triplet of quadrupole lenses used at the SLC. This 5 m long 6 ton assembly was kinematically supported on five roller cams. It is remotely adjustable in five degrees of freedom: pitch and yaw as well as horizontal and vertical displacement and roll. The rear three cams are of the same geometry as the ones described in this paper. The two front cams serve only to move that end of the barrel horizontally and vertically.

3. Hardware Realization

3.1 Shafts, Bearings, and V- and U-Blocks

The main components of a mover are sketched in Figs. 1 and 2. A magnet is fitted with two V-blocks and one U-block. The V-blocks are mounted on one side of the magnet and each rides on a pair of bearings mounted on the long camshafts. These enable any combination of vertical and horizontal motion. The U-block forms a flat surface which rides on the lone bearing on the short camshaft; this enables vertical motion and fixes roll α. In all cases, the cam lift is 1.5875 ± 0.010 mm,[8] and the cam diameter is 25 mm. Commercially-available hardened steel ball-bearings with a 62.00 ± 0.010 mm outside diameter were press-fit onto each camshaft. The short camshaft is 50 mm long, and the two long camshafts are 400 mm long. Eccentric cams were machined at the ends of each shaft. Angular twist between cams at opposite ends of a shaft was held to ± 1.6 mrad. This tolerance is critical to insure magnet motion is free from pitch and yaw. Flats were machined on the shafts to provide a reference surface from which the rotational tolerances could be controlled and measured. The shafts are made of hardened steel, and were fabricated to the desired tolerances by a computer-controlled precision grinding machine. The V-blocks and U-blocks are also made of hardened steel, and were fabricated on a computer-controlled milling machine to a tolerance of ± 0.01 mm.

3.2 Stepping Motors and Controllers, Gear-Boxes, and Potentiometers

Stepping motors drive each camshaft through a "harmonic drive" gear-box. The motors are mounted on aluminum housings which are themselves mounted on an aluminum base plate (the "T-plate" in Fig. 2). The stepping motors[9] require 400 steps for a complete rotation.[10] A holding current is supplied to one or two phases of each motor to achieve reliable single step motion and to avoid drift due to the weight of the magnet. The motors provide a holding torque of 0.025 N $\cdot$ cm

with one phase on. The gear-boxes[11] have a gear ratio 100:1 and transfer the stepping motor torque to the shafts without slip. The single step angle increment for each cam is 0.157 mrad.

A standard driver system designed for the SLC is used to operate the stepping motors. Several 48 channel magnet mover controller CAMAC modules are used in combination with 16 channel stepping motor drivers.[12] The motor driver system is configured to supply the holding current to the motor phases and also 10V DC to a rotary potentiometer ("pot") that is fixed to each cam at the end opposite to the stepping motor. The precision rotary pots[13] are single turn infinite resolution cermet type. The voltage output of the pots is read out through a 16 channel Smart Analog Module (SAM).[12] The 10V signal sent to the pots through the motor driver system is also picked off and put into a SAM channel. Variations of this voltage from the reference 10V are monitored at the same time the pots are read, and the pot readings are corrected for any fluctuation in line voltage.

The rotary pots are used to determine a magnet's midrange position and to check that a motor is responding with approximately the correct number of steps it has been commanded to move. The midrange position was determined by first starting with all shafts on the mover at their point of minimum lift, with the cam centers being directly below the shaft centers. The flats on the shafts were machined so that they face straight up at this position. The motors were then commanded to move (+10000,-15000,+15000) steps. When this movement was finished, the positions of the bearing centers with respect to the shaft centers were as shown in Fig. 1; this is the mover midrange position. The pots were then adjusted so that they read approximately 5V. The exact potentiometer voltages were recorded in a computer database. To return a magnet to its midrange position, the motors are stepped until all pots have returned to these values.

3.3 LVDTs, Electronics, and Calibration

From previous experience with magnet movers at SLAC, it was felt best to have a direct read-back of the magnet position, rather than rely on the shaft potentiometer read-back and the mover equations to determine the magnet location. Linear Variable Differential Transformers (LVDTs) were chosen for their resolution (essentially determined by the number of bits in the read-out ADC and the LVDT range of travel), their linearity (in principle $< 0.15\%$), and their ease of use. The LVDTs we used[14] were selected for their 5 mm full range, radiation hardness, and convenient spring-loaded, ball-contact package. The read-out we chose[15] conditions and reads back eight LVDTs with a 16 bit ADC in a single width CAMAC module. The least count resolution of this LVDT system is 0.18 μm.

There are three LVDTs per magnet. Two vertical LVDTs ($LVDT_1$ and $LVDT_2$) and one horizontal LVDT ($LVDT_3$) measure displacements of the magnet from its midrange position. The orientation and location of these LVDTs are shown in Fig. 7. With the magnet at its midrange position, the two vertical LVDTs are equally spaced on either side of $x = 0$ and are separated by a distance d_1. The horizontal LVDT is below the $y = 0$ axis by a distance d_2. For a standard FFTB quadrupole, the design dimensions were $d_1 = 164.1$ mm and $d_2 = 83.3$ mm. If all LVDTs are mounted in a transverse plane at z and monitor the motions of plane perpendicular (when $\alpha = 0$) magnet surfaces, then the location of the magnet center at that z is given by:

$$y = (L_1 + L_2)/2, \tag{2.1}$$

$$\alpha = \tan^{-1}\left(\frac{L_1 - L_2}{d_1}\right), \tag{2.2}$$

$$x = L_3 - (y + d_2)\tan\alpha, \tag{2.3}$$

where $\vec{L} = (L_1, L_2, L_3)$ are the differences of the LVDT readings from what they would read if the magnet was at its midrange position. Of course, the conditions

put forward for these equations were not met exactly in the movers we built. The consequences of this will be discussed in the section on calibration and testing.

3.3.1 LVDT Noise and Offsets

To reduce electrical noise, the LVDTs are read back over the longest processing time available in the Highland read-out modules (225 msec per LVDT). In addition to proper electrical grounding, we found noise in the LVDT system was most affected by environmental mechanical vibrations. With a mover on an isolation table in the lab or on the specially designed Anocast supports[16] on which the magnet and mover sit in the FFTB, we measured a *r.m.s.* LVDT noise of 0.5-0.9 least counts, or about 0.15 μm equiv. We also found that, in the absence of temperature variations, the measured value of a properly attached LVDT on an unmoved magnet changed little (a few counts) over a period of days. However, long term absolute stability of the LVDT system is not an integral requirement of the magnet positioning system. The magnet at its midrange position is still defined by the same reference voltages on the pots as when the shafts were first oriented to their proper positions. The mover LVDT system is "calibrated" by moving the magnet until all three pots read their reference voltages, and then reading the LVDT values. These values are taken as LVDT "offsets" and subtracted from all subsequent LVDT readings until the movers are re-calibrated, when a new set of constants is read in.

3.3.2 LVDT Linearity

The LVDTs used have a non-linearity specification of $< 0.15\%$ over their full range. This is loosely interpreted to mean that the worst residual to a straight-line fit relative to a perfect gauge would be < 8 μm over the LVDT full range of 5 mm. However, in the early stages of prototype testing, we found a much larger non-linearity in the mover motion, as determined by the LVDTs, when the mover was calibrated on a coordinate measuring machine (CMM).[17] This was traced to a

non-linearity in the combined LVDT plus read-out electronics. While the linearity of the ADC in the read-out module is better than 0.01%, the electronics were designed to read out a "ratiometric" LVDT, which reports two voltages for which the displacement of the LVDT is proportional to $\frac{(V_1-V_2)}{(V_1+V_2)}$. However, the LVDTs we used report voltages such that the displacement is proportional to $V_1 - V_2$, and offsets common to both V_1 and V_2 can and do occur. We then measured the reported displacement of a LVDT and the Highland read-out relative to a standard gauge[18] over a range of 4 mm. The residuals of a straight-line fit of gauge reading vs LVDT reading are shown in Fig. 8a. A simple cubic is sufficient to describe this non-linearity. The SLC control system was already set up to convert LVDT readings to displacements with up to a fifth-order polynomial, so it was possible to remove the non-linearity by calibration. We calibrated each LVDT, fitted each calibration to a cubic polynomial, and entered the coefficients of this fit into the SLC database for that LVDT.[19] Figure 8b shows an example of the residuals for gauge reading vs LVDT displacement after the correction. This shows sufficiently linear behavior. As a further check, a ratiometric LVDT[20] was measured vs the gauge using the standard (Highland) electronics, and a standard non-ratiometric (Daytronics) LVDT vs the gauge using read-out electronics manufactured by Daytronics. The residuals to *linear* fits are shown in Fig. 8c and 8d, respectively. Both show acceptable linear behavior without the need for a cubic correction. We also calibrated one standard LVDT using different channels of one Highland module, several different Highland modules, and several different lengths of cable from the LVDT to the module. This was done to make sure the coefficients were not a function of the combined LVDT plus electronics (which would have required pairing LVDTs, cables, and electronics channel at calibration), but instead were a simple property of the LVDT. Within statistics, the coefficients were a property only of the LVDT. With the cubic coefficients determined for a particular LVDT following it around in the SLC database, the full system was then linear to $< 0.1\%$.[21]

3.4 z Restraint

Early in the testing of the prototype mover a "drifting" problem was observed. When the mover with a magnet was subjected to repetitive motion tests (of the type described in the next section) and the cams were returned to positions they had previously been set to, the LVDTs would report that the magnet was at a slightly different position than it was the last time the cams were at that position (as determined by the pots). These shifts were small but they were all in the same direction, so that after a few hundred cycles, the magnet could be 30 or 40 μm away from where it had been the first time the magnet was moved to that position. Since, as will be described, the magnet position will ultimately be based on the LVDT readings, this effect in itself was not a major design flaw. However, it was also observed that if the LVDTs were monitored for a period of hours after the repetitive motion tests were finished, one could observe the magnet slowly drifting back to the position it was originally set to at the beginning of the repetitive motion tests. This was unacceptable, in that it meant that after motion, the movers might have to be continuously monitored and adjusted to keep the magnet fixed at its desired position.

While there is some settling-in of a magnet newly placed on a mover, this generally occurs in the first few tens of motions of the magnet and then stops. Simple tests allowed us to rule out this explanation, along with others relating to the LVDTs, stepping motors, and pots. The self-aligning spherical bearings used on the prototype mover were replaced with fixed-race bearings. While the fixed-race bearing did not solve the drifting problem, they were eventually used on the production movers.

The problem was eventually traced down to the U-block rubbing against the aluminum housing which shielded the lone cam (Cam 1). The U-block had been made a close sliding fit in this housing to fix the magnet's z position. The U-block would ride up against one side or the other of the housing, and this would introduce a small amount of hysteresis in the magnet motion. When the repetitive

motion was stopped, the force of gravity would slowly pull the magnet back to its original position. This is one example of the utility of having the magnet position determined by the LVDTs and not the pots.

This problem was solved by opening up the gap in the metal housing and using a turnbuckle to constrain the magnet's z position. This turn-buckle was ~ 9 inches long and was attached between a point in the (y, z) symmetry plane on the bottom of the magnet and the mover base plate after the magnet was set on the mover. It was then adjusted until the U-block was evenly spaced from either side of the housing with the mover at its midrange position. This arrangement solved the drifting problem, but it does couple the magnet transverse motion to a small motion in z, because the link pivots through an arc. Horizontal motion causes negligible (< 10 μm) z motion but maximum y motion can cause ~ 400 μm shifts in z position. However, this is well within the FFTB tolerance for positioning the magnet in z, and the effect can be easily and accurately modeled if knowledge of the exact z position of the magnet is needed.

3.5 Production and Quality Control

A total of 32 magnet movers were fabricated for the FFTB at MPI-Munich after one prototype had been made at SLAC. After a magnet mover had been completely assembled, and checked out for mechanical and electrical integrity, a series of tests were performed to commission the mover and to verify the tolerances. The test were carried out on a precision table in a room with temperature held constant to ± 0.5°C.

First the flats on the camshafts were adjusted so that the magnet, a FFTB standard quadrupole, was mounted in its midrange position. The electronic noise of the three LVDTs was measured by taking 30 readings each without moving the magnet. The standard deviation of these readings had to be less than two LVDT least counts. The magnet was then put through vertical, horizontal, and rotational movements to verify the proper functioning of the mover. These movements also helped settle the magnet in on the mover.

Finally the mover was subject to a two-hour endurance test, during which the magnet was moved up 480μm, down 960μm, and then back to 0. These motions were achieved by sending a predetermined number of steps to each motor, so the LVDTs and pots acted as independent verification of the mover motion. At each position (up, down, and midrange) the LVDTs and potentiometers were read out. The coefficients of the potentiometers were measured from these data and compared with the allowed range of 257.5 ± 2.5 μV/step. The reproducibility of moving to each position was required to be better than 1 μm as measured by LVDT_1 and LVDT_2, which measure the vertical movement. LVDT_3 measured any (unexpected) horizontal motion. Averaging over all movers, their positioning reproducibility can be summarized globally as $< \sigma_{vertical} >= 0.38$ μm and $< \sigma_{horizontal} >= 0.43$ μm, whereby the worst case is about a factor two larger than these averages.

For seven of the movers, the cam lifts for the three cams were measured using the same LVDT. The standard deviation of these 3×7 measured lifts was 9.8 μm.

4. Control System

Computer control of the magnet movers is very simple. The magnet is positioned by successive approximations. A desired position of the magnet ($\vec{x}_{DES}$) is entered. The angles ($\vec{\theta}_{DES}$) that the cams should be turned to reach this $\vec{x}_{DES}$ are then calculated according to Eq. 1. Before the magnet is moved, the three LVDTs are read in. This data gives the magnet's actual position in LVDT space ($\vec{L}_{ACT}$). $\vec{L}_{ACT}$ is transformed into $\vec{x}_{ACT}$ in MAG space according to Eq. 2, and from there into $\vec{\theta}_{ACT}$ in CAM space according to Eq. 1. The difference $\vec{\theta}_{DIFF} = \vec{\theta}_{DES} - \vec{\theta}_{ACT}$ is then calculated, and this gives the angular magnitude and sign the shafts need to turn to move an ideal magnet on an ideal mover from $\vec{x}_{ACT}$ to $\vec{x}_{DES}$. The number of steps each motor needs to take are then calculated and the CAMAC commands are sent out to step the motors. When the motors are finished, the LVDTs are read again, and the new $\vec{L}_{ACT}$ is transformed into a new $\vec{x}_{ACT}$. If $|\vec{x}_{ACT} - \vec{x}_{DES}| < \vec{\epsilon}$, where $\vec{\epsilon}$ is a predetermined tolerance in MAG space, then the magnet move is com-

plete. If $|\vec{x}_{ACT} - \vec{x}_{DES}| > \vec{\epsilon}$, then a new $\vec{\theta}_{ACT}$ is calculated and the motors are moved the number of steps indicated by $\vec{\theta}_{DIFF}$. This continues until $|\vec{x}_{ACT} - \vec{x}_{DES}| < \vec{\epsilon}$ or too many iterations have been taken, indicating a problem with the mover getting to $\vec{x}_{DES}$. For moves within 1 mm of the midrange position, it generally takes ≤ 4 iterations to reach $\vec{x}_{DES}$ within a tolerance of $\vec{\epsilon} = (1\mu\text{m}, 1\mu\text{m}, 2\mu\text{rad})$. Moves to the edges of the accessible area or over long distances (say 3 mm) may take twice as many iterations. More than 10 iterations almost always indicates a problem with the mover (a motor not working, a noisy LVDT, ...) or, if the $\vec{x}_{DES}$ is at an edge of the accessible region, an imperfection in the mover or model which has shifted the edge of the real accessible region away from the ideal one.

It should be noted that relying on the LVDTs to determine $\vec{x}_{ACT}$ removes much of the reliance on the model connecting MAG space to CAM space, and with it the exact tolerances of many of the mechanical parts, and on the linearity of the pots. In fact, except for certain diagnostic functions (is a motor responding or is it broken?) and for determining the midrange position, the pots on the shafts are not used to position a magnet. Similarly, as long as the MAG to CAM model is approximately correct (to a few percent), and as long as the stepping motors respond correctly to commands (including single-step commands) most of the time, precise sub-μm motion of the movers is possible without having built the movers to exacting tolerances. The linearity and reproducibility of the LVDT system has been established, so the question of accuracy of magnet motion reduces to how well the transformation from LVDT space to MAG space given in Eq. 2 holds. While the mechanism requires no great mechanical precision such as pitch uniformity in a lead screw, smooth hysteresis-free motion must be intrinsic to the mover if the LVDT feedback loop is to converge.

5. Mover Tests and Calibration

5.1 Positioning Accuracy

As a design goal, we tried to keep the mover positioning tolerance to < 5 μm in x and y and < 50 μrad in roll. If the preconditions to Eq. 2 hold and a magnet is *not* rolled ($\alpha = 0$), then the position measurement is insensitive to misplacements of the LVDTs. Even if a magnet is rolled by 5000 μrad, a large fraction of its total range, a 1 mm misplacement of one of the vertical LVDTs results in a mismeasurement of the y position by 2.5 μm and the roll by 30 μrad, and a 1 mm misplacement of the horizontal LVDT results in a x mismeasurement of 5.0 μm. It is reasonably easy to place a LVDT to within a mm of where it should be.

It is the failure to meet the preconditions to Eq. 2 that resulted in the most noticeable imperfections in magnet placement. The first precondition, that the LVDTs all be in the same transverse plane, could not met because, as can be seen in Fig. 7, LVDT_2 and LVDT_3 would interfere with each other. The two vertical LVDTs are kept in the plane with the magnet z center, and so the measurements of y and α, which do not depend on the reading of the LVDT_3 (see Eq. 2), correspond to those of the magnet z center. The horizontal LVDT could not even be mounted adjacent to LVDT_2, as this would have interfered with the operation of the lone cam bearing and U-block. It was mounted on top of the lone camshaft aluminum housing a distance $d_3 = 60$ mm from the magnet z center. This means that Eq. 2.3 is, in reality,

$$x = L_3 - (y + d_2)\tan\alpha - d_3 \tan\psi, \tag{3}$$

where ψ is the *unmeasured* yaw of the magnet. An unobserved yaw of 100 μrad in the mover will result in an error of 6 μm in the position of the magnet center in x. This will be illustrated when we discuss the mover calibration fixture.

The other precondition to Eq. 2 is that the LVDTs contact surfaces on the magnet that are plane (to a few μm) and perpendicular to the LVDT measurement

direction when the mover is at its midrange position. Not much forethought was given to the surfaces the LVDT probes contact. While the tolerances on machining the magnet pole pieces and split-planes were quite tight, the magnet outer surfaces (on which the LVDTs ride) do not affect the field quality in the bore, and so were manufactured to very loose tolerances. The outer surfaces were not parallel to the magnet split-planes, and these angles varied greatly between magnets. The surface finish was clearly not what was required, and in addition was painted. The low-cost solution to the surface quality problem we adopted was to scrape the paint off the magnet in the area around where the LVDTs would contact and glue tempered glass slides to the magnet. If undamaged, these slides have about the needed surface quality.

Even with the LVDTs riding on glass slides, we were still left with the fact that the surfaces are not perpendicular to the LVDT measurement directions. It is easiest to see this effect in LVDT space, in which the inverse of the transformation in Eq. 2 becomes:

$$L_1 = y + \frac{d_1}{2}\tan\alpha - x\tan\alpha_1, \tag{4.1}$$

$$L_2 = y - \frac{d_1}{2}\tan\alpha - x\tan\alpha_2, \tag{4.2}$$

$$L_3 = x + (d_2 + y)\tan\alpha + y\tan\alpha_3, \tag{4.3}$$

where α_i is the angle of the surface the ith LVDT rides on, with respect to the normal to the LVDT measurement direction, when the mover is at its midrange position. For the case where all $\alpha_i = 0$, the transformation in Eq. 2 is easily recovered. For the case where all α_i have the same magnitude *and sign*, the magnet coordinates in Eq. 4 are related to those in Eq. 2 by a simple rotation. Like a mover not being level on its Anocast stand, the mover roll control could compensate for this, though with some loss of mover range in x and y (see Fig. 5). However, these two simple cases were rarely seen with the FFTB quadrupole magnets.

It is possible to calibrate the α_i from the mover position residuals, which in this case are the real magnet positions minus the positions as determined by the LVDTs using Eq. 2. By moving the magnet in x along the $y = 0$ axis, α_1 and α_2 could be determined. If the difference of these two angles ($\alpha_D = \alpha_1 - \alpha_2$) is not zero, then there will be a residual in the x direction. α_D actually causes a roll residual as the magnet is moved in x, but as LVDT$_3$ is offset from $y = 0$, this causes an apparent x residual also. If the average of the two angles ($\alpha_A = \frac{\alpha_1+\alpha_2}{2}$) is not zero, then there will be a residual in the y direction as the magnet is moved along the $y = 0$ axis. These residuals are (by definition) zero at $x = 0$ and grow linearly as the x displacement of the magnet increases. A residual in the x direction as the magnet is moved in y along the $x = 0$ axis is the result of a non-zero α_3. All that was needed was a reliable measurement of the magnet position with about the same resolution of the mover LVDT system.

5.1.1 Mover Calibration Fixture

It would have been very time-consuming to mount, measure, and dismount each mover from the magnet fiducialization system[22] on the CMM, though one mover was kept mounted on the CMM for convenience of fiducializing magnets. Laser interferometers are precise and simple to use, but they excel in measuring displacements in the direction of the laser beam only when displacements transverse to the beam are small, and that was not the case for this application.

Our solution to the measurement problem was to build a special fixture to measure the movers. Given their ease of use and our experience with them, we used properly calibrated LVDTs of the same type used on the mover on this fixture. A magnet and mover were first married together on an Anocast stand. This was done before the magnet was fiducialized, which meant that the Kelvar tooling-ball fixtures (see Fig. 3), which were mounted on the magnet and which transferred the coordinate system defined by the magnet split-planes to easily accessible tooling-balls on the outside of the Kelvar fixtures, were not yet in place. This meant that the magnet split-planes were still accessible.

Our special measurement fixture was a rigid aluminum frame which was lowered onto the magnet and mover from above and bolted in place on the Anocast stand. It had three LVDTs which came down with the frame and touched horizontal split-planes from above. An arm was then bolted onto one side of the fixture which carried two LVDTs which touched vertical split-planes. Like the mover LVDTs, the fixture LVDTs were adjusted and had their offsets read for future subtraction when the mover was at its midrange position. With these five LVDTs, the values of the five degrees of freedom of the magnet (x, y, the roll α, the yaw ψ, and the pitch ϕ) could be determined (the magnet is constrained in z by the turn-buckle). The symmetric placement of the slots in the quadrupole iron which allowed access to the split-planes resulted in a very easy transformation from the fixture coordinate system to the magnet coordinate system. Two of the LVDTs touching horizontal split-planes were in a plane parallel to the mover (x, y) plane, and were symmetrically placed about the mover (y, z) plane. The difference these two LVDTs measured the roll of the magnet. One of these two LVDTs was in a plane parallel to the mover (y, z) plane with the third LVDT touching a horizontal split-plane, so the difference of these two measured the pitch of the magnet. These two LVDTs were equidistant from the mover (x, y) plane, so their average gave the magnet y position at the intersection of their plane with the mover (x, y) plane, and with the already determined roll, this was easily translated to y in the magnet coordinate system. Similarly, the two LVDTs touching vertical split planes were in a plane parallel to the mover (x, z) plane, equidistant from the (x, y) plane, and so their difference measured the magnet yaw, and their average, properly corrected for measured roll, gave x in the magnet coordinate system.

Using the SLC control program performing stand-alone CAMAC commands, we designed automated programs to scan the magnet position. We moved the magnet from -2 mm to $+2$ mm in 500 μm steps in x along the $y = 0$ axis and measured the x and y residuals between the mover and fixture positions. α_A and α_D were calculated from least-square straight line fits to the residuals as a function of mover x, and α_1 and α_2 were derived from these. These were put into the new

LVDT space to MAG space transformation (the inverse of Eq. 4), and then the magnet was scanned in y along the $x = 0$ axis from -1.5 mm to $+1.5$ mm in 500 μm steps. The value for α_3 was then derived from a straight line fit to the x residual as a function of y motion.

It generally took three series of scans to reach convergence for the α_i for a magnet and mover pair. In Fig. 9 is an example of the x and y residuals for the initial and final scans along the x axis for the worst (in terms of LVDT surface angles) of the FFTB quadrupole magnets. For the initial scan, $\alpha_i = (0, 0, 0)$. This scan shows residuals on the order of $30 - 40$ μm at the ends of the mover range. For the final scan, $\alpha_i = (-4212, -34484, -2082)$ μrad were derived from previous scans and used in the transformation. The x and y residuals for this scan were within the tolerance of ± 5 μm over the full mover range. We were able to measure α_i to get all movers except one within this tolerance. The average magnitudes of α_A, α_D, and α_3 were all on the order of 5 mrad.

As mentioned, one mover could not be brought within tolerance solely by measuring its α_i and adding them to the transformation. This "worst" mover was investigated in more detail. Two different types of devices were used to independently verify the LVDT-based mover and fixture measurement systems; magnetic encoder displacement (SONY) gauges[23] with a precision of 1 μm, and a laser-interferometer system with retroreflectors,[24] with a precision of 0.1 μm. As Fig. 10a shows, while the y residuals during a x scan were well within tolerance, the x residual grew to $\sim 25\mu$m at the negative end of its range (for $x < -1800$ μm, the mover is out of tolerance). The best measured values of $\alpha_i = (-2434, -2846, -3015)$ μrad have already been included in the transformation, and the scan step size has been reduced to 200 μm to more clearly show the effect. Since the residuals due to α_i should grow linearly with displacement, this is clearly *not* the problem with this mover. The yaw, pitch, and roll residuals are shown in Fig. 10b, and it is obvious that the magnet was also yawing by ~ 100 μrad at the end of its range. While a yaw around the y axis at $z = 0$ cannot by itself result in the observed x displacement through Eq. 3, a yaw around some other point along the z axis will translate

to a yaw around $z = 0$ and a x displacement. The laser interferometer measured in x at $z = 0$, and essentially confirms the fixture measurement (Fig. 10d). The SONY gauges (Fig. 10c) also measured x and were placed on either side of the laser retroreflector in z. Their average confirmed the fixture and laser x residuals, and their difference measured a yaw of ~ 100 μrad, confirming the fixture yaw observation. Clearly the magnet is yawing, probably due to a mechanical tolerance not being met, and $LVDT_3$, in correcting for the added displacement at its z position, was introducing a large displacement at the magnet center. It should be reiterated that out of 33 movers, only one showed flaws of this magnitude.

5.2 Incremental Motion

Movers which have good positioning accuracy have many applications. They can be used as stages and compared to, or used to augment, other systems such as BPMs, wire alignment systems or laser alignment systems, which may or may not have good position information. However, this is not the design function of these movers. Even with worse positioning accuracy than described in the previous section, the first few coarse steps of beam-based alignment would bring a magnet to within ~ 50 μm of its desired position. What is needed is precise incremental motion from this point, so that the beam-based alignment procedures will converge quickly. Effects such as LVDT non-linearity, or the surface rotations described in the previous section, are small on these distances. Lost steps can be detected in the LVDT system and corrected for, though very many will slow precision motion and so need to be avoided.

We performed numerous test to verify the precise incremental motion of the movers. Most mover motion is quite involved, requiring all three motors to turn different numbers of steps. Simple motion of one motor results in motion in all three magnet degrees of freedom. However, there is one subset of motor sequences that results in simple motion, and these can be used to illustrate the precision of the movers. Motion along the x axis from the midrange position requires only Cams 2 and 3 to turn an equal number of steps in the same direction. The minimum

step size for this motion is 0.35 μm, for a command of (0,1,1) steps sent to the motors.[25] Another nice feature of this motion is that, since $\alpha = 0$, $LVDT_3$ directly measures the x position of the magnet.

Figure 11 shows a test where we sent out a series of thirty (0,1,1) step commands to the motors, followed by a (0,-30,-30) step command to return the mover to $x = 0$. The solid line shows the position the mover should be at after each command. Since the LVDTs were not used to position the magnet in this test, $LVDT_3$ was read out after each command and gave the x position of the magnet. These are the data points in Fig. 11. As an independent check, the laser interferometer was also set up to read the x position of the magnet between each command. The position as measured by the laser is the dotted line in Fig. 11. As can be seen, the mover can execute sub-μm motion quite reliably.

Since the steps were all in the same direction in the previous test, they do not address the question of mover backlash. To investigate this, we sent a series of three (0,1,1) step commands to a mover, followed by three (0,-1,-1) step commands, for a total of four cycles. This command sequence is shown as the solid line in Fig. 12. Once again, $LVDT_3$ (data points) and the laser interferometer (dotted line) were read back after every command. While the tracking is not perfect, we are measuring motions near the resolution of the measuring devices, and the magnet does not show any significant backlash at the $\sim 1\mu$m level.

6. Temperature Behavior

The magnets and movers are made of steel, iron, and aluminum. Temperature behavior at the μm scale can be quite involved, depending on factors such as tunnel temperature, or magnet current, versus time. The center of the magnet moves from 0.5 to 2 μm/°C,[26] and the LVDTs on the movers do not track this motion exactly. The temperature dependence of several of the LVDTs was measured[27] and found to be $(-0.88 \times (T - 20))$ μm at T = 20°C. Thus it is clearly important to keep the operational temperature constant to within ~ 1°C if one wants motions

reproducible at the μm level. Before operation of the FFTB, the tunnel is sealed and the fans are turned off. This helps stabilize the temperature in the part of the tunnel not in direct sunlight to better than 1°C. The temperature of the magnets (and eventually of the movers) can change by $\sim$ 25°C when they are turned on and ramped to full current, so this is done well in advance of beam-based alignment. Aligning the quadrupoles requires scanning the magnet currents by a significant fraction of their design values. They are scanned quickly and the magnets are returned to their nominal currents in less than a minute, so the heat load on the magnet and mover does not change substantially.

7. Conclusions

We have constructed precision magnet mover out of easily machined parts and commercially available instrumentation. At constant temperature, these movers have a positioning accuracy of ± 5 μm and a incremental positioning precision of $\sim$ 0.4 μm, with backlash at the $<$ 1 μm level. Difficulties encountered in the development stage, such as LVDT non-linearity and LVDT surface angles, were easily worked around.

The magnet movers have been used during the 1994 FFTB runs, and their performance has been very satisfactory.[28] Certain unforseen functions, such as calibration of the wire alignment system,[29] have been taken up by the mover system due to their accuracy, reliability, and ease of use.

It was originally envisioned to measure the misalignment of the sextupoles by scanning their currents and observing changes in the beam size at the primary focus (IP) of the FFTB,[30] and then use the movers to correct the magnet positions. It turned out to be easier to scan the positions of the magnets with the movers, and directly find the positions which minimize the effects of misalignment. The result of such a scan is shown in Fig. 13, where the beam position at a downbeam BPM is shown as a function of sextupole x position. The scatter of the points at a particular x is a reflection of the jitter of the incoming beam. It was quite easy

to determine the offset of the magnetic center of the sextupole shown in Fig. 13 to an accuracy of 7 μm, and to move it the 220 μm necessary to center it on the beam line. This method is preferable to scanning the sextupole currents, as it avoid hysteresis effects in the magnet iron and possible loss of standardization. Another advantage of this method is that it only requires the BPM system, and does not rely on the beam size monitors at the FFTB IP. It is not possible to align quadrupoles with this technique, as the deflection of the trajectory changes sign at the magnetic center, and no extremum appears.

It has also been possible to design "knobs" which change the position of the beam x and y waists and dispersions at the FFTB IP, and the $x'y$ coupling, by purposely offsetting sets of sextupoles by calculated amounts.[30] This technique has better accuracy and precision than the originally envisioned quadrupole strength knobs. The quadrupoles can also be moved prescribed amount to induce precise kicks to the beam. This can take the place of corrector dipoles for functions such as lattice diagnostics, and in general there has been no need to use the FFTB corrector dipoles. These functions are all possible because of the positioning accuracy of the movers.

7.1 Recommendations for Improvements for NLC Movers

In designing the next generation of magnet movers for a NLC, the movers should be considered part of the magnet/BPM system from the very start. They should be mated together early, intercalibrated with respect to each other, and treated as a complete unit.

Care should be taken when the magnets are produced to make sure the surfaces the LVDTs will ride on are at specific angles (nominally but not required to be zero) with respect to the magnet split-planes, and to make sure the surface quality of the LVDT surfaces is sufficient. With modern precision milling machines, this should not be difficult, as the total area needed for a LVDT surface is $<$ 1 cm^2.

If it can be afforded, it is probably best to equip a mover with five LVDTs. If

care is taken with the symmetrical placement of LVDTs around the mover, then the transformation from LVDT space to the position of the magnet center can be made very simple, as was the case with our calibration fixture. Even with no mover control of yaw and pitch, this would give passive monitoring of them and make sure that uncontrolled (but acceptable from the point of view of beam optics) yaw and pitch did not introduce an unknown systematic error in the accurate placement of the magnet, as is possible (at a small level) with our movers. If only three LVDTs can be afforded per mover, then they should all be placed at the z center of the magnet. For our movers, this would have meant building an arm which attached to the base plate outside of the paired cams and held the horizontal LVDT above the cams. This would not have been a much more involved than the arrangement we used, and it could have reduced or eliminated d_2 in Eq. 2. Care should be taken early in the design stage to place the LVDT holders where they are easily accessible and to design LVDT holders that are easy to adjust; this will save much integrated time later.

In addition to magnet placement, these movers can be easily adapted to other beamline components which might need precision placement, such as RF cavities. One of the FFTB movers is currently being used to position the target box of the SLAC E144 experiment. The purpose of this experiment is to study nonlinear, very high field QED. The target is a terawatt laser pulse focused down to an area of a few tens of square microns, and the target box is an optical table which contains the final mirrors. Having the optical table on a mover allows positioning of the target with respect to the FFTB beam at the μm level.

If component placement is needed only to an accuracy of > 10 μm, then it is possible to imagine designing movers with no LVDTs which relied only on the pots on the cam shafts for positioning, as was done for the original SLC final triplets. However, it is always possible for a magnet to become decoupled from its mover for any number of unforseen reasons, and the hours or days of expensive beam time spent diagnosing these problems can often easily pay for a good LVDT system which would make the problem immediately apparent.

We ended up having to calibrate each LVDT by hand. However, unless one plans to buy the LVDTs and their read-out from the same manufacturer and then blindly trust their calibration, it is advisable to make arrangements to do this on your own. Using a third order polynomial in place of a single linear coefficient, which we were forced to do, allowed us to do slightly better than the advertised linearity of the LVDT system.

A more careful job of calibrating the movers could have probably resulted in a linearity of the system down to 0.0010, but this was not needed for the FFTB and so was not pursued. To reach this level, certain problems we ignored, such as LVDT transverse backlash, would need to be addressed. To do much better than that with this type of stage and calibration would be difficult. As it was, we achieved a linearity of ~ 0.0025 at constant temperature. Being able to reach this so easily is probably a function of the simplicity and symmetry of the mover design, and these features should be retained.

Acknowledgements:

Many people contributed to the successful completion of this project with their time and effort. At SLAC, we would like to thank Ed Askeland, Mike Browne, Bernie Denton, Karl Bouldin, Dave Burke, Peter Tenenbaum, and Bill Wagner. The mover project was initiated by the late Gerry Fischer, a world expert on accelerator magnets, alignment, and ground motion. We would like to dedicate this paper in his memory. Dave Sawyer was responsible for the conception and design of the mover calibration fixture. At MPI, we would like to thank Robert Richter, Helmut Schmücker, Horst Stieg, the late Ulrich Stierlin, and Jenny Thomas. We would also like to thank John Larkin at Highland Technology for help with the LVDT system.

REFERENCES

1. R. B. Palmer, Annu. Rev. Nucl. Part. Sci. 40 (1990), 529.
2. Final Focus Test Beam Project Design Report, SLAC-Report-376, March 1991, Stanford Linear Accelerator Center, Stanford University, Stanford, California 94309.
3. D. L. Burke, "Results from the Final Focus Test Beam," SLAC-PUB-6609, to be published in the proceedings of the Fourth European Particle Accelerator Conference, London, England, June 27–July 1, 1994.
4. H. Hayano *et al*, Nucl. Instr. Meth. **A320** (1992) 47.
5. The standard definition of z being in the direction of the beam and y being vertically up is used.
6. A. Bergamin, G. Cavagnero, and G. Mana, Rev. Sci. Instr. 64 (1993), 168
7. J. E. Furse, J. Phys. Sci. Instr. 14 (1981), 264.
8. The *mechanical* tolerance is indicated by the $\pm$-sign in this subsection.
9. Model M061LS02 stepping motor, Superior Electric, Bristol, CT 06010.
10. The motors are run in a "half-step" mode of operation to achieve the desired resolution.
11. Model 1C Harmonic Drive, Quincy Technologies, Wakefield, MA 01880.
12. SLC Control System Hardware Manual, Stanford Linear Accelerator Center, Stanford, CA 94309.
13. Series 6670 cermet potentiometer, Beckman Industrial, Fullerton, CA
14. Model DS190A LVDT, Daytronics Corp, Miamisburg, OH 45342
15. Model M550 LVDT scanner, Highland Technology, San Francisco, CA 94122
16. Anocast, a division of Anorad Corp., Hauppauge, NY 11788.

17. Mitutoyo C Series 806-10 coordinate measuring machine, MTI Corp, Paramus, NJ 07652.
18. Model 755 height gauge, with a read-out accuracy of 1 μm, Starrett L. S. Co., Athol, MA 01331.
19. While the coefficients varied between LVDTs, the first-order coefficient was typically $+0.177$ $\mu\mathrm{m}/count$, the second-order coefficient was typically -144×10^{-6} $\mu\mathrm{m}/count^2$, and the third-order coefficient was typically $+111 \times 10^{-6}$ $\mu\mathrm{m}/count^3$.
20. Schaevitz Corporation, Pennsauken, NJ 08110
21. Highland Technology now makes a variant on their LVDT scanner designed to read out non-ratiometric LVDTs of the type manufactured by Daytronics.
22. G. E. Fischer et al, "Precision Fiducialization of Transport Components," SLAC-PUB-5764, contributed to the 3rd European Particle Accelerator Conference, Berlin, Germany, March 24-28, 1992.
23. SONY Magnescale Inc., Orange, CA 92665.
24. Model 5528A laser interferometer, Hewett-Packard, Palo Alto, CA
25. This step size is for motion near the midrange position. The minimum step size actually becomes much smaller near the edges of the mover range.
26. Klaus Flöttmann, private communication
27. G. Heimlinger, "Untersuchung von Präzisionsmechanik für zukünftige 500 GeV e^+e^- Linear-Collider," Technischen Universität München Diplomarbeit, MPI-PhE 93-13, June 1993
28. V. Balakin et. al., "Focusing of Sub-micron Beams for TeV-Scale e^+e^- Linear Colliders," Phys. Rev. Lett. **74** (1995) 2479.
29. V. E. Bressler et al, "Overview of the Final Focus Test Beam Alignment System," SLAC-PUB-6194, contributed to the Particle Accelerator Conference, Washington DC, May 17-20, 1993.

30. P. Emma et al, "Beam Based Alignment of the SLC Final Focus Sextupoles," SLAC-PUB-6209, contributed to the Particle Accelerator Conference, Washington DC, May 17-20, 1993.

FIGURE CAPTIONS

1) Schematic drawing of a mover at its midrange position supporting a standard FFTB quadrupole magnet. The various dimensions and coordinate systems are described in the text.

2) Perspective drawing of a FFTB quadrupole magnet being placed on a mover.

3) Two quadrupole magnets and movers (in foreground) sit on their Anocast stands immediately after installation on the FFTB beamline. LVDT_1 is visible just behind the front V-block and Camshafts 2 and 3 on the mover in front. The Kelvar tooling ball fixtures (described in text and marked CAUTION DO NOT TOUCH in photo) are in place, but the FFTB wire alignment system, the sensors for which are supported off these fixtures, is not yet installed.

4) Range of motion for a magnet on a mover.

5) Ranges of motion in the (x, y) plane with mover roll set to (a) zero, (b) $\alpha = 1000$ μrad, (c) $\alpha = 5000$ μrad, and (d) $\alpha = 9550$ μrad.

6) Perspective drawing of the barrel containing the final triplet of quadrupole magnets used in the first phase of SLC running, on a five cam mover.

7) Orientation and location of mover LVDTs.

8) The fit residuals (with respect to the Starrett height gauge) vs. LVDT displacement for (a) Daytronics LVDT, Highland electronics, and a linear fit, (b) Daytronics LVDT, Highland electronics, and a cubic fit, (c) Schaevitz LVDT, Highland electronics, and a linear fit, and (d) Daytronics LVDT, Daytronics electronics, and a linear fit.

9) The residuals (with respect to the measurement fixture) vs. mover x position (with $y = \alpha = 0$) for the mover with the largest LVDT surface angles. The square symbols connected by solid lines represent the initial scan with $\alpha_i = (0, 0, 0)$. The circle symbols connected by dashed lines represent the

final scan, with $\alpha_i = (-4212, -34484, -2082)$ μrad used in the LVDT to MAG transformation. The x (y) residuals are the filled (open) symbols.

10) The residuals vs. mover x position for the one mover which failed to meet the positioning tolerance requirements: (a) the x and y residuals with respect to the measurement fixture, (b) the yaw, pitch, and roll residuals w.r.t. the fixture, (c) the x residuals w.r.t. the SONY gauges, and (d) the x residual w.r.t. the laser interferometer. The dashed lines are the nominal tolerances for deviation from ideal behavior.

11) A sequence of thirty (0,1,1) step commands were sent to a mover, followed by a (0,-30,-30) step command. The solid line shows the expected motion of the magnet, the data points show the x position as measured by $LVDT_3$ (the other 2 LVDTs showed no significant y motion or roll), and the dashed line shows the x position as measured by the laser interferometer.

12) A sequence of three (0,1,1) step commands were sent to a mover, followed by three (0,-1,-1) step commands, for a total of four cycles. The solid line shows the expected motion of the magnet, the data points show the x position as measured by $LVDT_3$, and the dashed line shows the x position as measured by the laser interferometer.

13) The electron beam x position measured at a downbeam BPM vs. an upbeam sextupole mover x position. The scatter of the points at a particular sextupole x is a reflection of the jitter of the incoming beam. The curve is a parabolic fit to the data, used to determine the misalignment of the sextupole from the nominal beamline.

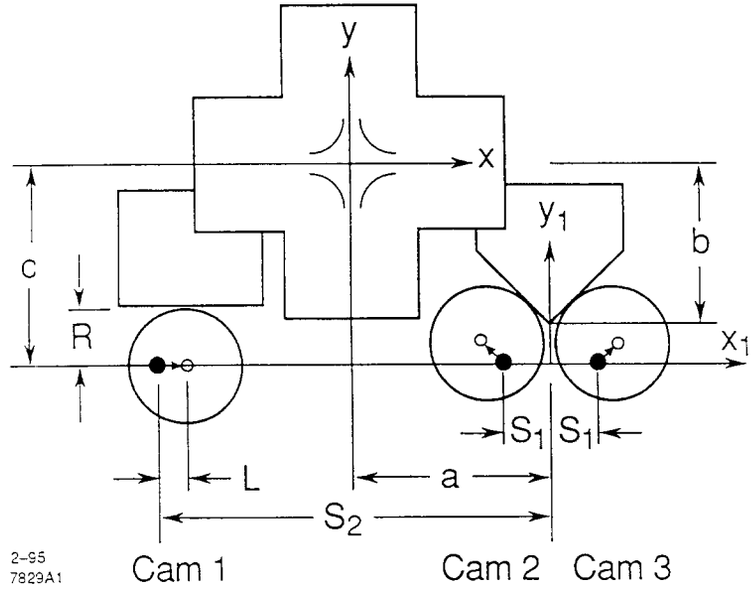

Figure 1

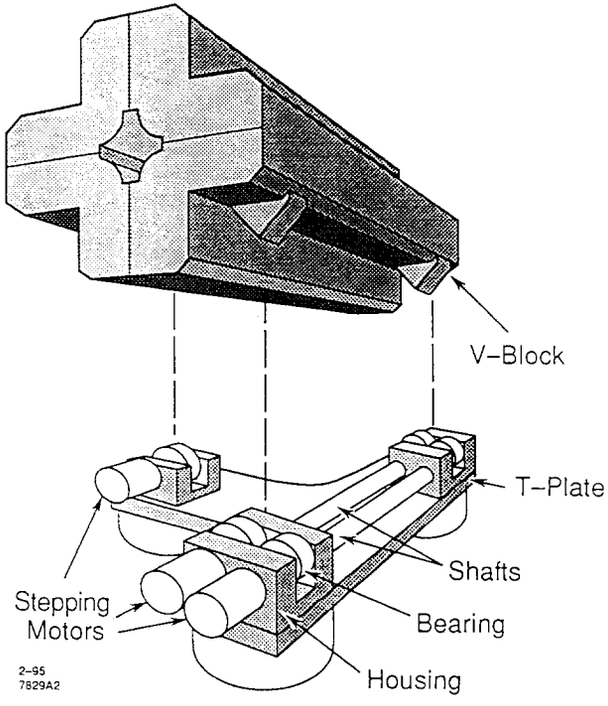

Figure 2

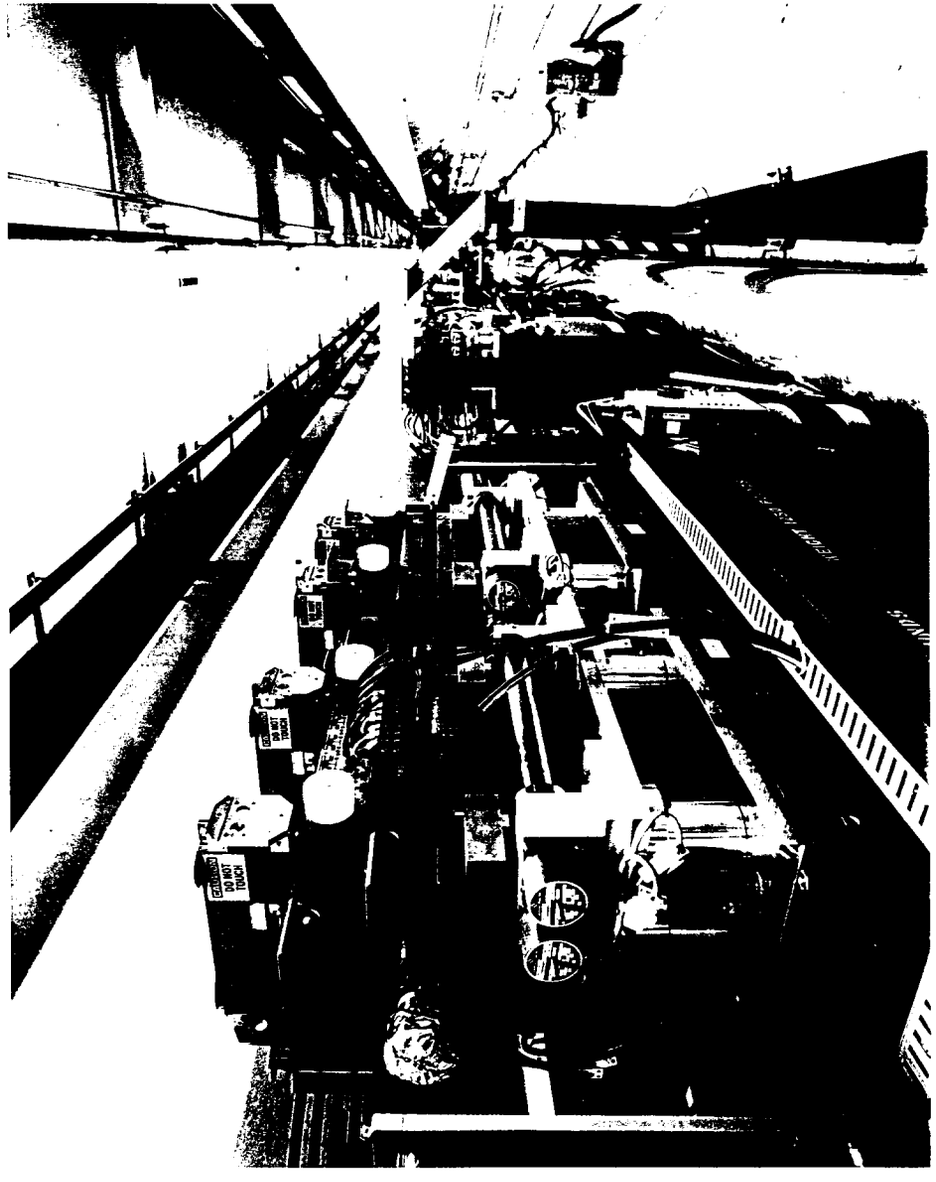

Figure 3

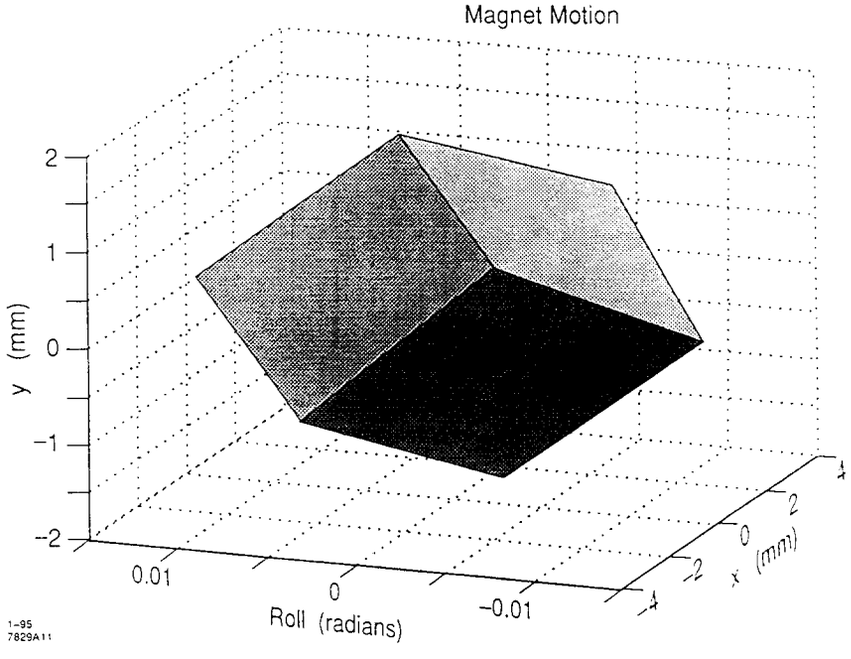

Figure 4

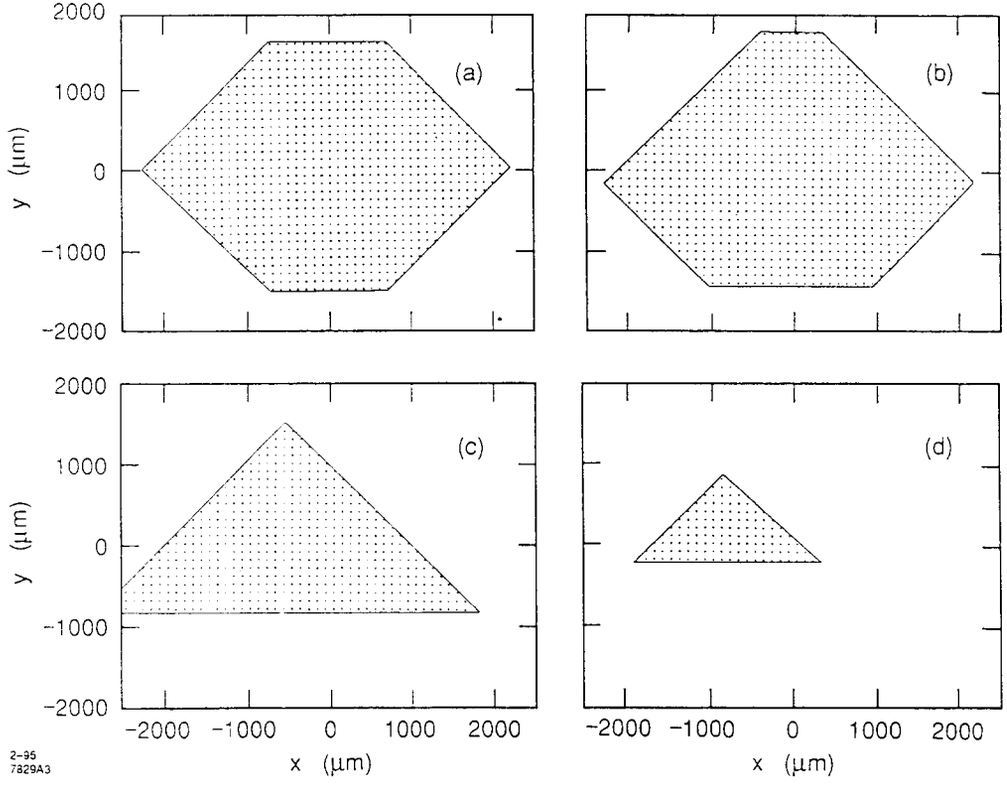

Figure 5

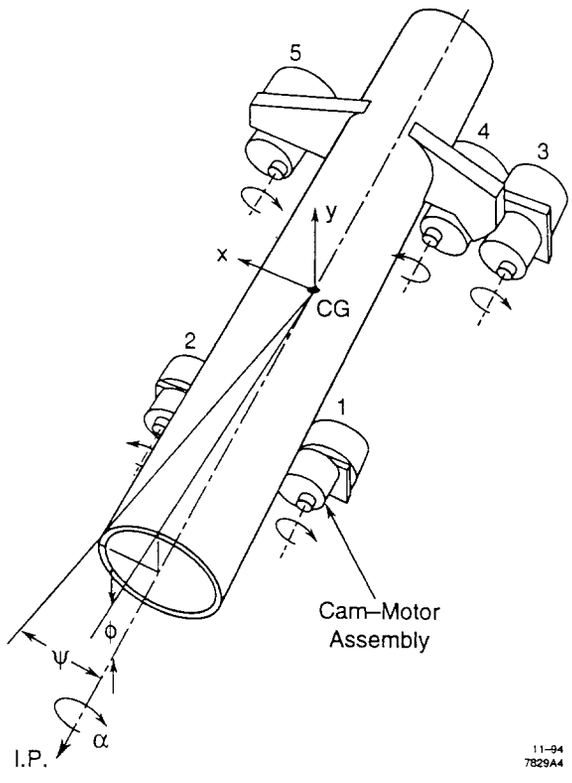

Figure 6

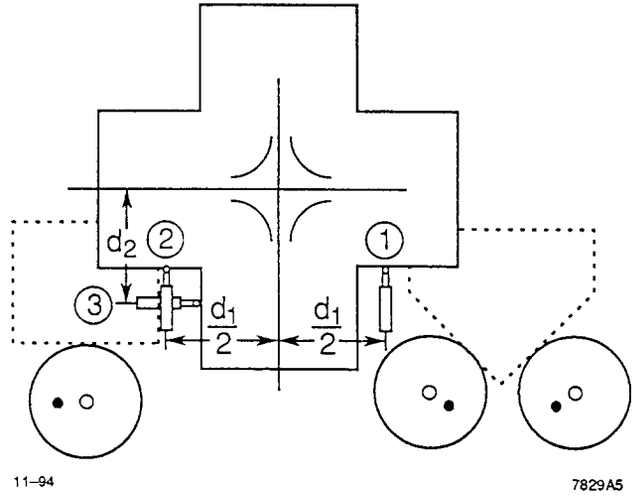

Figure 7

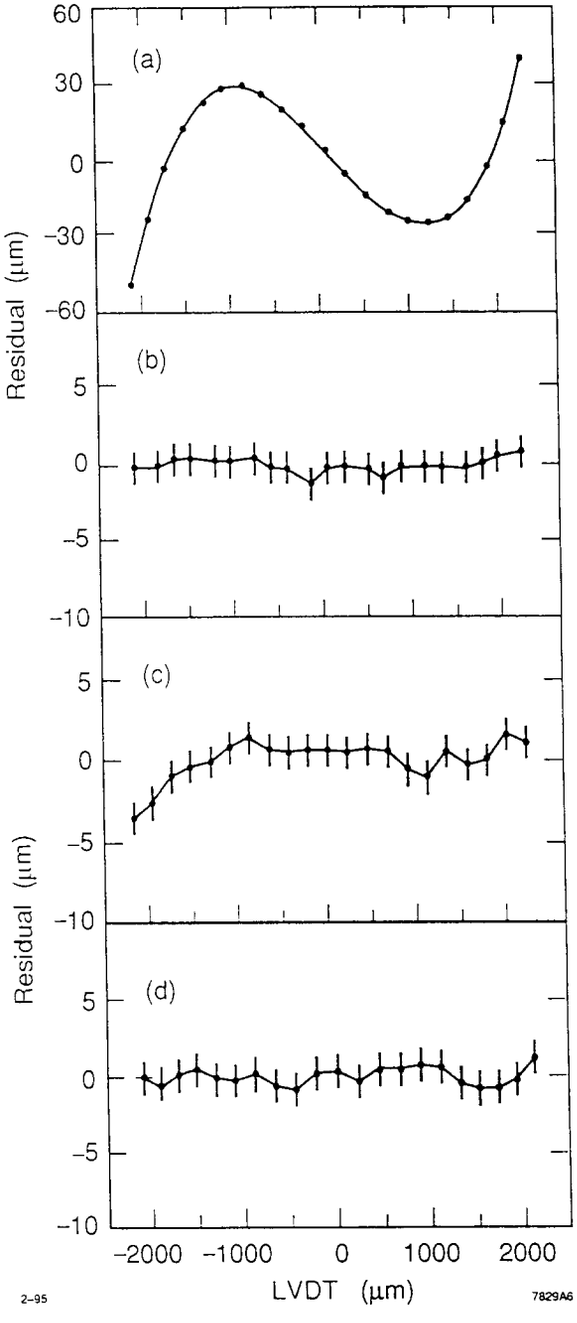

Figure 8

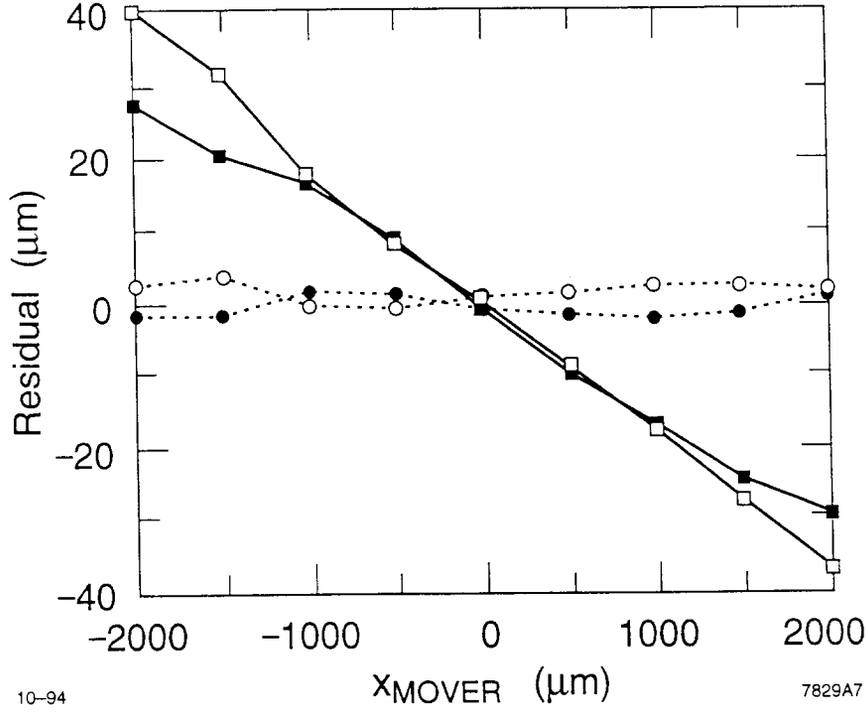

Figure 9

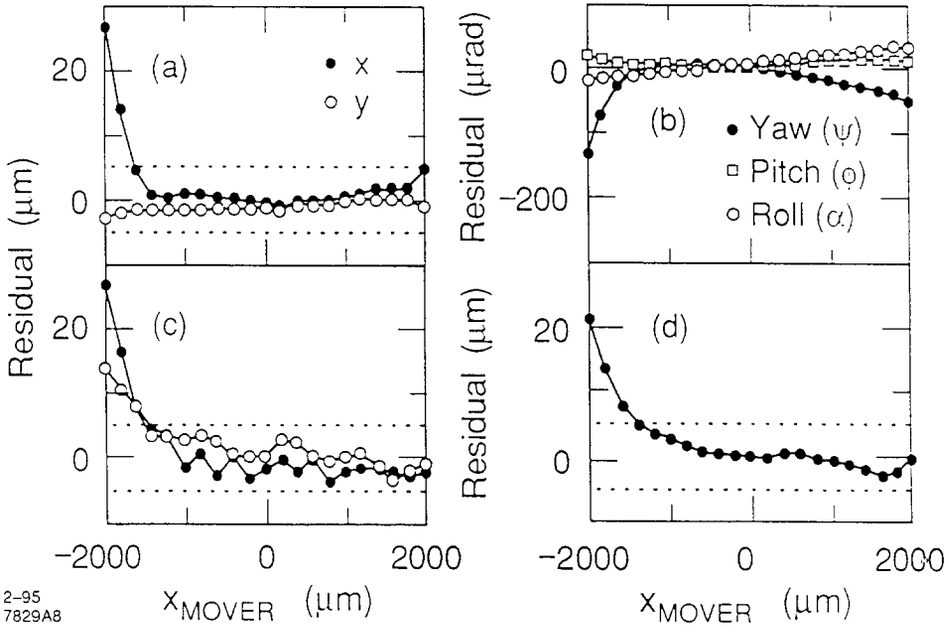

Figure 10

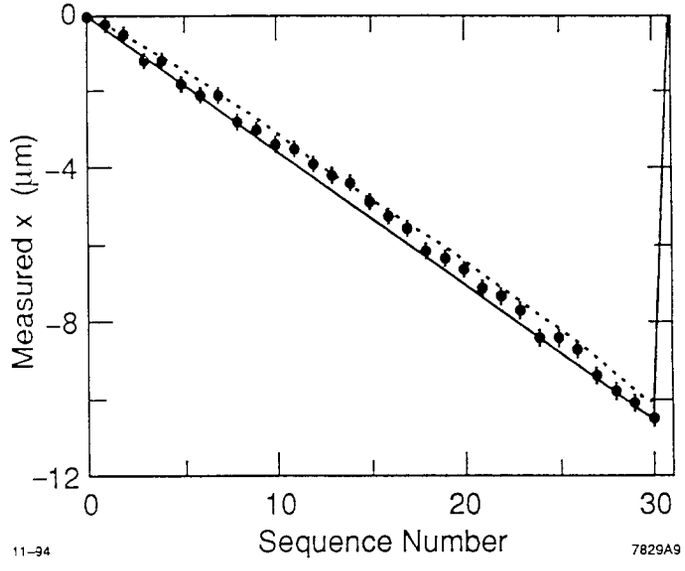

Figure 11

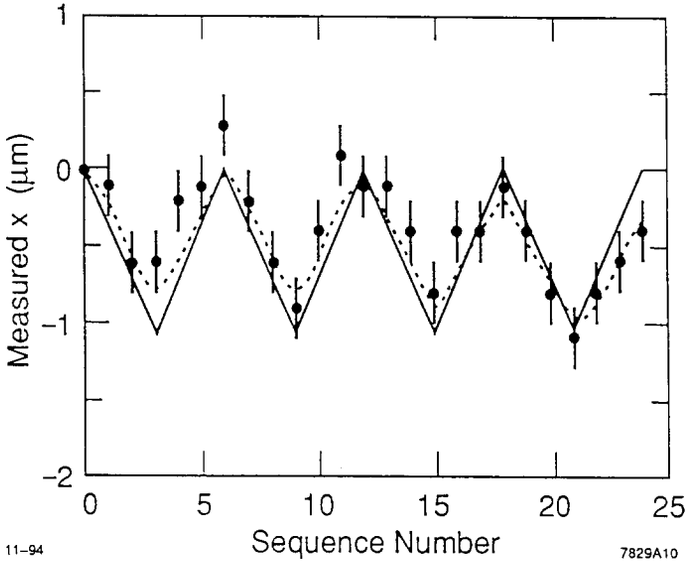

Figure 12

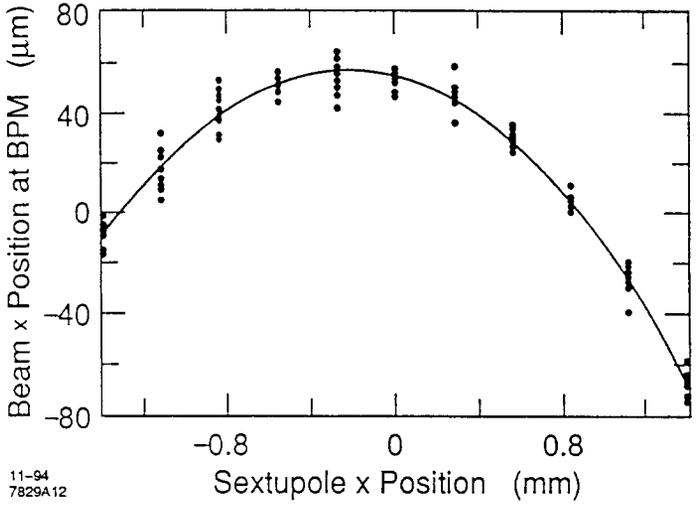

Figure 13